SOLUTION OF THE NITROXIDE SPIN-LABEL SPECTRAL OVERLAP PROBLEM USING PULSE ELECTRON SPIN RESONANCE

JUN-JIE YIN, JIM B. FEIX, AND JAMES S. HYDE
National Biomedical Electron Spin Resonance Center, Department of Radiology, Medical College of Wisconsin, Milwaukee, Wisconsin 53226

ABSTRACT Short-pulse saturation-recovery (SR) electron spin resonance (ESR) methods have been used to measure the lateral diffusion of a nitroxide-labeled cholesterol analogue (3-spiro-[2′-(*N*-oxyl-4′,4′-dimethyloxazoladine)]-cholestane, CSL) in multilamellar liposomal dispersions. SR experiments were performed on samples containing ^{14}NCSL:^{15}NCSL pairs, and recovery signals were analyzed for initial conditions and multiexponential time constants by computer simulation. Rate equations describing the system were written and solved. The time constants contain combinations of electron spin lattice relaxation times T_{1e} for both isotopes and the Heisenberg exchange rate constant K_x. We have investigated the complication that occurs from overlap of ESR spectral fragments from ^{14}N and ^{15}N moieties. The time constants of the multiexponential signals are independent of ESR line shape and position. From K_x, lateral diffusion constants of CSL in dimyristoylphosphatidylcholine (DMPC) were calculated ($D = 1.7 \times 10^{-8}$ at 27°C and 2.7×10^{-8} cm^2/s at 37°C). It is shown that short-pulse saturation-recovery methods are able to overcome the ESR spectral overlap problem that is encountered in conventional ESR and continuous wave electron–electron double resonance (CW ELDOR) studies of spin–spin interactions. The present method can be extended to more complex situations involving spin labels in different environments with physical and chemical exchange.

INTRODUCTION

In the first nitroxide radical spin-label paper, Hubbell and McConnell (1) encountered a problem that has continued to bother practitioners of the method. The spin label Tempo (2,2,6,6-tetramethylpiperidine-1-oxyl) partitions into lipid bilayers such that signals of similar intensity from labels in the aqueous and lipid phase are observed. The signals strongly overlap and the problem was to obtain information on the rate of interchange of Tempo between the two environments. The difficulty lay in accurate simulations of spectra. The line shapes exhibited a mixture of homogeneous and inhomogeneous character (from unresolved couplings to methyl protons). The distribution of spectral differences between the labels in the two environments leads to a distribution of exchange effects in the composite spectra.

A similar problem was encountered in membrane-protein systems where signals from spin-labeled bulk lipids and spin-labeled boundary lipids are superimposed and strongly overlapped (2–4). In this case the boundary lipid signal is from lipids that are slowly tumbling. It would be difficult to make a convincing argument concerning the exchange rate from spectral analysis, because the motional model for the lipid is in doubt. Both the Tempo partition problem and the boundary-lipid problem are examples of physical exchange.

Another overlap problem arises in the case of Heisenberg exchange in spin-labeled lipid bilayers. The problem of extracting the Heisenberg exchange rate by computer analysis of spectra from a spin label is made difficult because concentrations must be fairly high, which can alter the system under investigation, because the model for rotational motion is uncertain, and because of intermolecular dipolar interactions.

As an approach to solving the Heisenberg exchange problem, dual labels, i.e., labels with ^{14}N and labels with ^{15}N can be employed. If at least one feature, say that $M_I = 0$ line of ^{14}N, shows minimal overlap, the technical problems of extracting Heisenberg exchange information are reduced. One can obtain each spectrum separately, and observe changes when both labels are present. But quantitation remains difficult.

The above examples all depend on a spectral feature as expressed in radians per second being comparable to an exchange rate. They are "T_2-sensitive" methods. In this laboratory we have been developing a variety of "T_1-sensitive" methods where the exchange rate is comparable with T_1^{-1}. Because T_1s are at least two orders of magnitude longer than T_2s, much slower processes can be studied. But

an overlap problem also is encountered. Feix et al. (5) developed the ^{14}N–^{15}N spin-label pair continuous wave electron–electron double resonance (CW ELDOR)[1] method. Reliable exchange rates could be obtained in the T_1 time scale if at least one spectral feature had no overlap from the two isotopic species. But they avoided situations where there was overlap because of concern that ELDOR effects between isotopic species could not be separated from ELDOR effects within an isotopic species. Thus no data were presented in their work for exchange rates between spin-labeled membrane constituents in the situation where both ^{14}N and ^{15}N spectra were in the slow-tumbling domain.

The nitroxide spin-label overlap problem, as shown in this introduction, has multiple aspects that arise from the complicated nature of the spectra. To a good approximation, saturation-recovery pulse electron spin resonance (ESR) methods depend only on the time evolution of the z-component of magnetization. We have recently shown (6–8) that superimposed multiple exponentials are observed when short saturating microwave pulses are delivered to a spin system. The time constants of these exponentials contain both saturation transfer and longitudinal relaxation rates. The quality of the data is so high and the number of experimental controls sufficiently large that one can reliably deconvolute triple exponentials. It is suggested in these papers that even more complex saturation-recovery signals can be deconvoluted.

In the present paper we show that the methods developed by us can be extended theoretically to the situation where there is spectral overlap. We show that the time constants of the multiple exponential saturation-recovery signal are independent of the degree of spectral overlap. Only the prefactors are affected. This is a general solution of the spectral overlap problem. We demonstrate the method by using ^{14}N and ^{15}N cholestane spin-label pairs in a lipid bilayer. To the extent that cholestane is accepted as an analogue for cholesterol, this is one of the first measurements of lateral diffusion of cholesterol (9–11).

THEORY

The basic idea and the theoretical structure including energy diagrams, rate equations, and the initial short pulse condition are based on our previous work (6–8). The main difference is that here we consider a system in which the ESR spectra of the probes overlap, whereas previously the spectra were well-resolved.

In this work, two isotopes are employed. If the hyperfine lines are strongly coupled by nitrogen nuclear relaxation, which we show later to be a good approximation for cholestane spin-label pairs in dimyristoylphosphatidylcholine (DMPC) above the main phase transition temperature, this is the case of model I in reference 6 (Fig. 1 *b*). The appropriate energy level diagram is the same but the superimposed ESR spectrum is quite different. Fig. 1 shows the spectrum of the two cholestane spin probes exhibiting various degree of overlap.

Because of the fast nitrogen nuclear relaxation, it is sufficient in the energy-level diagram to combine the hyperfine transitions for each isotope into single transitions for the purpose of calculating saturation-recovery signals. Spin-lattice relaxation couples both spin systems to the lattice and Heisenberg exchange couples them together.

Assume (*a*) W_{12} is the electron spin-lattice relaxation rate of ^{14}NCSL. (*b*) W_{34} is the electron spin-lattice relaxation rate of ^{15}NCSL. (*c*) K_x is the Heisenberg spin exchange rate constant between ^{14}NCSL and ^{15}NCSL spin label pairs where 3-spiro-(*Z'* = [*N*-oxyl-4', 4'-dimethyloxazoladine])-cholestane (CSL) stands for cholestane spin label.

Using the same theoretical structure as in reference 6, the rate equations are

$$\frac{d}{dt}[(n_1 - n_2) - (N_1 - N_2)] = -2W_{12}[(n_1 - n_2) - (N_1 - N_2)] + 2K_x(n_2n_3 - n_1n_4), \quad (1)$$

$$\frac{d}{dt}[(n_3 - n_4) - (N_3 - N_4)] = -2W_{34}[(n_3 - n_4) - (N_3 - N_4)] - 2K_x(n_2n_3 - n_1n_4), \quad (2)$$

where $n_{1,2,3,4}$ represent the instantaneous populations per unit volume of the four levels and $N_{1,2,3,4}$ represent the equilibrium Boltzman populations per unit volume.

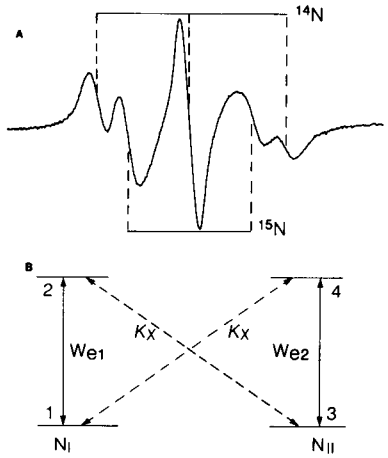

FIGURE 1 (*A*) ESR spectra. ^{14}NCSL:^{15}NCSL (0.5:0.25 mol%) cholesterol analogue spin probes in DMPC at 37°C, pH 9.5 (*B*) The relaxation model. Because of very fast nuclear relaxation, hyperfine lines of each isotope are assumed to be strongly coupled.

[1] *Abbreviations used in this paper:* CSL, 3-spiro-(2'-[*N*-oxyl-4', 4'-dimethyloxazoladine])-cholestane; CW ELDOR, continuous wave electron–electron double resonance; DMPC, dimyristoylphosphatidylcholine; ESR, electron spin resonance; SR, saturation recovery; W_{Hex}, Heisenberg spin exchange frequency (i.e., collison frequency involving paramagnetic species).

Let N_I and N_{II} be the concentrations of ^{14}NCSL and ^{15}NCSL, respectively ($n_1 + n_2 = N_I$; $n_3 + n_4 = N_{II}$).

The observable signals are $i_1 = (n_1 - n_2) - (N_1 - N_2)$; $i_2 = (n_3 - n_4) - (N_3 - N_4)$.

The differences of Boltzman distribution of spin I $(N_1 - N_2)$ and spin II, $(N_3 - N_4)$ are proportional to the concentrations of these spin species, namely, $(N_1 - N_2) = cN_I$ and $(N_3 - N_4) = cN_{II}$ (c is a constant).

From reference 6 the general solutions for the observable signals are

$$i_1 = I_1 e^{-(A-B)t} + I_2 e^{-(A+B)t}, \tag{3}$$

$$i_2 = I_3 e^{-(A-B)t} + I_4 e^{-(A+B)t}, \tag{4}$$

where

$$A = W_{12} + W_{34} + (1/2)K_x(N_I + N_{II}), \tag{5}$$

$$B = [(W_{12} - W_{34})^2 - K_x(N_I - N_{II})(W_{12} - W_{34}) + (1/4)K_x^2(N_I + N_{II})^2]^{1/2}, \tag{6}$$

and $I_{1,2,3,4}$ are coefficients to be defined by initial conditions. Quite generally a double exponential is observed.

There are some relations between the coefficients of the two exponentials.

$$\frac{I_3}{I_1} = \frac{N_{II}K_x}{\ell}, \tag{7}$$

$$\frac{I_4}{I_2} = \frac{N_{II}K_x}{m}, \tag{8}$$

where

$$\ell = -(A - B) + 2W_{12} + 2W_{34} + N_I K_x, \tag{9}$$

$$m = -(A + B) + 2W_{12} + 2W_{34} + N_I K_x. \tag{10}$$

Eqs. 3, 4, 7, and 8 give physical insight into the effects of the intermolecular interactions in the two spin systems.

Eqs. 1 and 2 and the solution Eqs. 3 and 4 are in fact a complete and sufficient proof of the thesis of this paper. Overlap affects initial conditions but cannot affect time constants. Detected signals in the case of overlap are some combinations of i_1 and i_2, and again, time constants are not affected. It is instructive nevertheless to analyze the effects of overlap on the prefactors, and this analysis constitutes the remainder of the theoretical portion of this paper.

We previously have studied the interaction between unlike spins using short pulse techniques where the ESR spectra of the two different spins were well separated. In this case if spin system I is pumped, i_1 is the saturation-recovery signal and i_2 is the pluse ELDOR signal.

In saturation-recovery studies with overlap we must consider (a) the preparation of the spin system by the saturating pulse and (b) the resulting composite saturation-recovery signal. At $t = 0$,

$$i_1 = (n_1 - n_2) - (N_1 - N_2) = \rho_1(N_1 - N_2) - (N_1 - N_2) = c(\rho_1 - 1)N_I, \tag{11}$$

$$i_2 = (n_3 - n_4) - (N_3 - N_4) = \rho_1(N_3 - N_4) - (N_3 - N_4) = c(\rho_2 - 1)N_{II}, \tag{12}$$

where

$$-1 \le \rho_1 \le 1 \text{ and } -1 \le \rho_2 \le 1. \tag{13}$$

If $\rho_{1,2} = -1$, spin systems I and II are totally reversed. If $\rho_{1,2} = 0$, spin systems I and II are fully saturated. If $\rho_{1,2} = 1$, spin systems and I and II have not been affected by the pumping field.

In the presence of spectral overlap, the saturation-recovery signal is the sum of i_1 and part of i_2, namely.

$$i_{SR} = i_1 + \rho_3 i_2 \quad 0 \le \rho_3 \le 1, \tag{14}$$

If $\rho_3 = 0$, the two ESR spectra are well separated. If $\rho_3 = 1$, the two ESR spectra are totally superimposed.

At $t = 0$, from Eqs. 3, 4, 7, 8, 12, and 13,

$$i_1 = I_1 + I_2 = c(\rho_1 - 1)N_I, \tag{15}$$

$$i_2 = I_3 + I_4 = \frac{N_{II}K_x}{\ell} I_1 + \frac{N_{II}K_x}{m} I_2 = c(\rho_2 - 1)N_{II}. \tag{16}$$

From Eqs. 16 and 17 we have

$$I_2 = \frac{(\rho_2 - 1)\ell + (1 - \rho_1)N_I K_x}{(1 - \rho_2)m + (\rho_1 - 1)N_I K_x} I_1. \tag{17}$$

Because $i_{SR} = i_1 + \rho_3 i_2$, the saturation-recovery signal is

$$i_{SR} = I_1\left[\left(1 + \frac{\rho_3 N_{II}K_x}{\ell}\right)e^{-(A-B)t} + \left(\frac{\rho_3 N_{II}K_x}{m} + 1\right) \cdot \left(\frac{(\rho_2 - 1)\ell + (1 - \rho_1)N_I K_x)}{(1 - \rho_2)m + (\rho_1 - 1)N_I K_x)}\right)e^{-(A+B)t}\right] \tag{18}$$

Eq. 18 gives the general solution for the saturation-recovery signal.The most remarkable feature is that the time constants of the double exponential remain the same; only the coefficients are changed when spectral overlap occurs.

The strategy we have developed here does not deal explicitly with the saturation parameter or the spectral overlap (namely the line-shape problem). We simply introduce three parameters, ρ_1, ρ_2 (which express the initial saturation), and ρ_3 (which expresses the population distributions) in our calculations. Without knowing these parameters quantitatively, from computer simulation we can directly obtain the intermolecular interaction rate constant between the unlike spins.

In the case where ^{14}NCSL and ^{15}NCSL spin labels are used, the labels are at the same position on the sterol backbone and have the same electron spin-lattice relaxation probability W_e to a good approximation (see Table I). Considerable simplification occurs. Eqs. 3 and 4 become

$$i_1 = I_1 e^{-2W_e t} + I_2 e^{[2W_e + K_x(N_I + N_{II})]t}, \tag{19}$$

$$i_2 = I_3 e^{-2W_e t} + I_4 e^{-[2W_e + K_x(N_I + N_{II})]t}, \tag{20}$$

TABLE I
ELECTRON SPIN-LATTICE RELAXATION TIMES FOR CSL

Temperature	T_{1e} ^{14}NCSL	T_{1e} ^{15}NCSL
°C	μs	μs
27	4.23 ± 0.08	4.62 ± 0.08
37	3.26 ± 0.08	3.64 ± 0.07

^{14}NCSL and ^{15}NCSL spin probes were present at 0.5 mol% in DMPC membranes, pH 9.5. Single exponential signals were obtained. Data come from computer simulations.

and Eqs. 7 and 8 become

$$I_3 = (N_{II}/N_I)I_1, \tag{21}$$

$$I_4 = -I_2. \tag{22}$$

For short pulse excitation conditions,

$$I_2 = \frac{\rho_1}{(1-\rho_1) + N_I/N_{II}} I_1 \tag{23}$$

and the saturation-recovery signal is

$$i_{SR} = i_1 + \rho_3 i_2 = I_1\left[\left(1 + \frac{N_{II}}{N_I}\rho_3\right)e^{-2W_e t} + (1-\rho_3) \cdot \frac{\rho_1}{(1-\rho_1) + N_I/N_{II}} e^{-2W_e + K_x(N_I+N_{II})t}\right]. \tag{24}$$

If the two ESR spectra are well separated, $\rho_1 = 0$, $\rho_2 = 1$, and $\rho_3 = 0$ and

$$i_{SR} = I_1\{e^{-2W_e t} + (N_{II}/N_I)e^{-[2W_e + K_x(N_I+N_{II})]t}\}. \tag{25}$$

This was encountered previously (6).

If the two ESR spectra are totally superimposed, $\rho_1 = 0$, $\rho_2 = 0$, and $\rho_3 = 1$, and

$$i_{SR} = I_1[1 + (N_{II}/N_I)]e^{-2W_e t}. \tag{26}$$

A single exponential is observed. Actually, this is just a single spin system with a different theoretical treatment.

MATERIALS AND METHODS

The ^{15}N nitroxide-labeled cholestane spin label, 3-spiro-(2′-[*N*-oxyl-4′, 4′-dimethyloxazoladine])-cholestane, designated here as ^{15}NCSL, was a gift from Prof. J. H. Park. ^{14}NCSL and DMPC were from Sigma Chemical Co., St. Louis, MO.

Stock solutions of spin labels and lipids were prepared in chloroform and stored at −20°C. The buffer was 0.1 M borate at pH 9.5. Multilamellar liposomes were prepared by directly hydrating the dried lipids and spin labels with an appropriate amount of buffer as described previously (6). All spectra were obtained using sample capillaries made of methylpentene polymer TPX (0.6 mm inside diameter). A flow of temperature-regulated nitrogen gas over the capillary was used to remove oxygen (12).

The CW ELDOR technique was used to estimate the ratio of the nuclear spin-lattice relaxation rate to the electron spin-lattice relaxation rate. The measurements were performed as described previously using a loop gap resonator (13). Both pumping and observing microwave frequencies were fed to the resonator. The measurements were made with the pumping frequency on resonator resonance and the observing frequency off resonance. This provides the best isolation of pumping and observing microwave fields. ELDOR experiments were performed as described previously (14). ELDOR reductions were measured on the center line of ^{14}N when the low field line was pumped. The separation was 40 MHz between the two microwave frequencies.

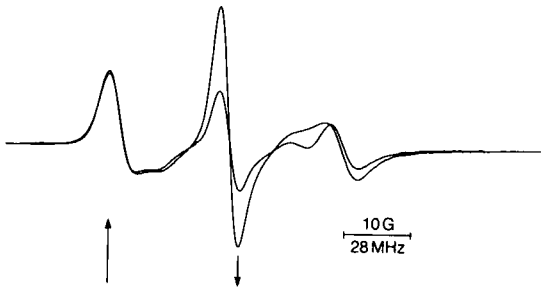

FIGURE 2. The ELDOR effect for ^{14}NCSL (0.1 mol%) cholesterol analogue spin probes in DMPC at pH 9.5. The ELDOR reduction (R_∞) is 85.5% at 27°C and 68.0% at 37°C. 100 kHz field modulation of 1.0 G amplitude was used.

The CW ELDOR reduction factors were determined at a series of nine pumping intensities and R^{-1} plotted against the inverse pumping power P^{-1} (15). Extrapolation to infinite pumping power gives the intercept R_∞^{-1}, which is a function of the relaxation processes occuring in the spin system. With a rather low spin-label concentration, the relaxation process is dominated by nuclear spin-lattice relaxation, and from reference 16,

$$R_\infty(\text{END}) = \frac{b + b^2}{1 + 3b + b^2}, \tag{27}$$

$$b = W_n/W_e. \tag{28}$$

The saturation-recovery spectrometer is based on the design of Huisjen and Hyde [17]. A multichannel signal acquisition system greatly improves the signal-to-noise ratio over what could be achieved with the single channel boxcar. A field-effect transistor (FET) microwave amplifier has been introduced. The time response limit is ~0.1 μs. A high-order low-pass filter at the input to the analogue/digital converter cuts off at 25 MHz, which results in minimal distortion of the transient signal. Typically, 2 × 10^4 decays per second are acquired with 512 data points on each

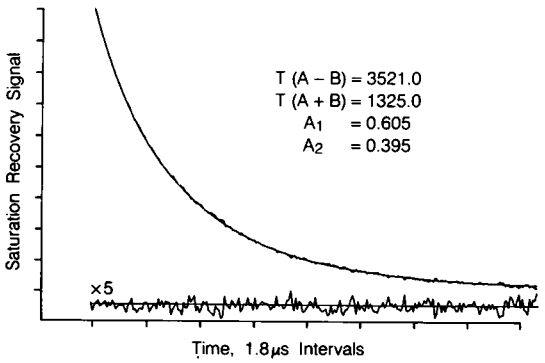

FIGURE 3. Saturation-recovery signal and curve fitting in computer simulation with mixed ^{14}NCSL and ^{15}NCSL (0.5:0.25 mol%) in DMPC at 37°C, pH 9.5. Data appear in Table II. Simulations and experimental saturation-recovery signal are superimposed. The difference multiplied by a factor of five is shown as the "residual." Each recovery signal obtained in 5 min at 20,000 accumulations per second, 512 data points per accumulation.

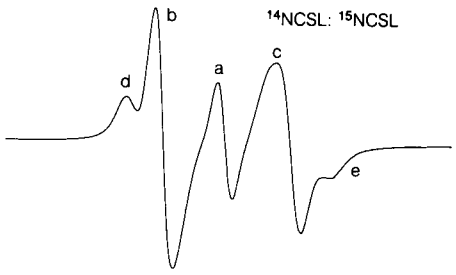

FIGURE 4 ESR spectra with mixed ^{14}NCSL and ^{15}NCSL (0.5:0.75 mol%) in DMPC at 37°C, pH 9.5. *a, b, c, d,* and *e* indicate positions in the ESR spectrum at which the data of Table III were obtained.

decay. Total accumulation time is ~5 min. Aperture intervals were 40 ns for 37°C and 60 ns at 27°C.

The short pulse saturation-recovery experiments were performed as in our previous study. As a control, every experiment was run with different pump durations, because the time constants of the multiexponential are independent of the width of the pump pulse (6, 7).

The theoretical models were compared with experimental saturation-recovery curves using the Monte Carlo approach for optimizing the fit (6). A least-squares minimization function was used as the criterion of excellence of the fit between model and experiments. The curve-fitting program was run alternatively on a PDP 11/34 or an IBM 9000 computer.

All samples were run with the buffer at pH 9.5 for comparison with our previous work. (Actually, there was no difference in the experimental data when the sample was in buffer of pH 7.5).

It is generally assumed that spin exchange is strong and K_x is equal to the collision rate constant. The lateral diffusion constant D can then be obtained using an appropriate model (18).

RESULTS AND DISCUSSION

Fig. 2 shows the CW ELDOR experimental results with ^{14}NCSL spin label in DMPC. From the ELDOR reductions R_∞, the ratio of nuclear spin-lattice relaxation rate to electron spin-lattice relaxation rate, b, was calculated using Eqs. 27 and 28. The results (b = 11.3 for 27°C and 3.8 for 37°C) show that W_n is much greater than W_e.

After a delay of ~ 2 μs to allow nuclear levels to equilibrate, single exponential decay curves were observed from either ^{14}NCSL or ^{15}NCSL spin probes alone in DMPC at 27 and 37°C, indicating that nuclear relaxation is the dominant intramolecular saturation-transfer mechanism under these experimental conditions. The three hyperfine lines of ^{14}NCSL and two hyperfine lines of ^{15}NCSL are strongly coupled by nuclear relaxation, and analysis of the tails of the SR experiment gives T_1. Table I gives the experimental data.

Fig. 3 shows a representative saturation-recovery signal with mixed ^{14}NCSL and ^{15}NCSL spin labels in DMPC. Eqs. 16–20 of reference 8 show that five exponentials are expected, three of which are very short in the presence of fast nuclear relaxation. The early portions (~2 μs) of the SR signals were cut off in the data analysis; the tails were double exponentials. The Heisenberg spin exchange rate constant, K_x, was calculated from the two time constants using Eq. 19. Fig. 4 shows a conventional ESR spectrum of mixed ^{14}NCSL and ^{15}NCSL spin labels in DMPC. The five different lines in the spectrum show spectral overlap in varying degrees. Saturation-recovery signals were obtained from the five different positions indicated in Fig. 4. The time constants of the double exponential remained the same for each of these positions; only the coefficients changed as predicted by our theory. Table II shows the experimental data.

Different combinations of the two spin-label concentrations result in different line shapes and different extent of spectral overlap. Table III shows that the spin-exchange rate constant K_x is invariant when the concentration of spin probes is changed.

For comparison to the previous work, the lateral diffu-

TABLE II
EXPERIMENTAL DECAY AND COLLISION RATE CONSTANTS VS. SPECTRAL POSITION

Line position	*a*	*b*	*c*	*d*	*e*
$T(A - B)$ (μs)	3.26 ± 0.08	3.23 ± 0.08	3.18 ± 0.08	3.30 ± 0.08	3.35 ± 0.08
$T(A + B)$ (μs)	1.12 ± 0.05	1.15 ± 0.05	1.16 ± 0.05	1.19 ± 0.05	1.13 ± 0.05
K_x (*MHz/mol*)	46.9	44.8	43.8	43.0	46.9

$T(A - B)$, $T(A + B)$ values were from computer simulations of experimental data of samples containing ^{14}NCSL and ^{15}NCSL (0.5:0.75 mol%) in DMPC at 37°C, pH 9.5. Here $T(A - B) = (2w_e)^{-1}$, $T(A + B) = [2W_e + (N_{II})K_x]^{-1}$. See Eq. 19.

TABLE III
EXPONENTIAL DECAY AND COLLISION RATE CONSTANTS VS. ^{15}NCSL CONCENTRATION

^{14}NCSL:^{15}NCSL/DMPC (*mol %*)	0.5:0.1	0.5:0.25	0.5:0.5	0.5:0.75
$T(A - B)$ (μs)	3.50 ± 0.08	3.35 ± 0.08	3.51 ± 0.08	3.28 ± 0.08
$T(A + B)$ (μs)	1.80 ± 0.05	1.53 ± 0.05	1.36 ± 0.05	1.12 ± 0.05
K_x (*MHz/mol*)	45.0	47.3	45.0	47.0

Experimental data was obtained at 37°C, pH 9.5. $T(A - B)$, $T(A + B)$ values are from computer simulations. Here $T(A - B) = (2w_e)^{-1}$, $T(A + B) = [2W_e + (N_I + N_{II})K_x]^{-1}$. See Eq. 19.

TABLE IV
LATERAL DIFFUSION CONSTANTS FOR CHOLESTANE SPIN LABEL

Temperature	K_x	D
°C	MHz/mol	$cm^2s^{-1} \times 10^8$
27	29.1	1.68
37	46.3	2.67

K_x values were calculated from Eq. 19. Lateral diffusion constants D were calculated from the Träuble and Sackmann equation (18).

sion constant, D, was calculated from K_x by using the Träuble and Sackmann equation (18). The lateral diffusion constants, D, are shown in Table IV. The calculated values for D are in excellent agreement with those reported for a fluorescent analogue of cholesterol in DMPC determined by photobleaching recovery (10). They also agree well with lateral diffusion constants for fluorescent analogues of phospholipids (10, 11, 19).

Cholesterol exerts considerable influence on the physical and dynamic properties of membranes (3, 20, 21), including the lateral diffusion of both protein and lipid component (10, 11, 19, 21). However, the lateral diffusion of cholesterol itself has only rarely been examined (9–11, 18). The significant body of information on the lateral phase separation of cholesterol has largely been inferred from the behavior of phospholipid analogues (9, 22–24) and the partitioning of Tempo (22). This has in part been due to the broad spectral features of available cholesterol-analogue spin labels. The capability to observe biomolecular collisions between ^{14}N and ^{15}N cholestane probes should allow more direct study of these problems.

CONCLUSIONS

More complicated problems where the assumption of fast nuclear relaxation and equal electron spin-lattice relaxation rates cannot be made will certainly arise in the future. The rate equations can be solved theoretically for these situations using matrix algebra techniques (8). Quite generally, the eigenvalues or time constants will always be independent of spectral overlap. If the multiple exponentials can be separated, the overlap problem appears solved. As indicated in our earlier papers, the high quality of the saturation-recovery data and the numerous experimental controls that are available demonstrate that this will often be possible.

There exists the possibility to improve the signal-to-noise ratio by using high observing powers, and this could be important in applying the methods discussed here to biological membranes. One would then need a more complete theoretical treatment than that provided by rate equations. The work of Percival and Hyde (25) and more recently Sugano et al. (26) can serve as guidelines in the development of such a theory.

We thank Professor J. H. Park for providing ^{15}N cholesterol analogue spin labels.

This work was supported by grants GM 27665, GM 22923, and RR 01008 from the National Institutes of Health.

Received for publication 10 September 1987 and in final form 30 November 1987.

REFERENCES

1. Hubbell, W. L., and H. M. McConnell. 1968. Spin-label studies of the excitable membranes of nerve and muscle. *Proc. Natl. Acad. Sci. USA.* 61:12–16.
2. Jost, P. C., K. K. Nadakavukaren, and O. H. Griffith, 1977. Phosphatidylcholine exchange between the boundary lipid and bilayer domains in cytochrome oxidase, containing membranes. *Biochemistry.* 16:3110–3114.
3. Devaux, P. F., and M. Seigneuret. 1985. Specificity of lipid-protein interactions as determined by spectroscopic techniques. *Biochim. Biophys. Acta.* 822:63–125.
4. Pates, R. D., and D. Marsh. 1987. Lipid mobility and order in bovine rod outer segment disk membranes. A spin-label study of lipid-protein interactions. *Biochemistry.* 26:29–39.
5. Feix, J. B., C. A. Popp, S. D. Venkataramu, A. H. Beth, J. H. Park, and J. S. Hyde. 1984. An electron-electron double resonance study on interaction between [^{14}N] and [^{15}N] stearic acid and vertical fluctuation in dimyristoylphosphatidylcholine. *Biochemistry.* 23:2293–2299.
6. Yin, J.-J. M. Pasenkiewicz-Gierula, and J. S. Hyde. 1987. Lateral diffusion of lipids in membrane by pulse saturation recovery electron spin resonance. *Proc. Natl. Acad. Sci. USA.* 84:964–968.
7. Yin. J.-J., and J. S. Hyde. 1987. Spin-label saturation-recovery electron spin resonance measurements of oxygen transport in membranes. *Z. Phys. Chem.* 153:S57–S65.
8. Yin. J.-J., and J. S. Hyde. 1987. Application of rate equations to ELDOR and saturation recovery experiments on ^{14}N:^{15}N spin label pairs. *J. Magnetic Resonance.* 74:82–93.
9. Sackmann, E., and H. Träuble. 1972. Studies of the crystalline-liquid cyrstalline phase transition of lipid model memgranes. II. Analysis of electron spin resonance spectra of steroid labels incorporate into lipid membranes. *J. Am. Chem. Soc.* 94:4492–4498.
10. Alecio, M. R., D. E. Golan, W. R. Veatch, and R. R. Rando. 1982. Use of a fluorescent cholesterol derivative to measure lateral mobility of cholesterol in membranes. *Proc. Natl. Acad. Sci. USA.* 79:5171–5174.
11. Golan, D. E., M. R. Alecio, W. R. Veatch, and R. R. Rando. 1984. Lateral mobility of phospholipid and cholesterol in the human erythrocyte membrane: effect of protein-lipid interaction. *Biochemistry.* 23:332–339.
12. Popp, C. A., and J. S. Hyde. 1981. Effects of oxygen on ESR spectra of nitroxide spin-label probes of model membranes. *J. Magnetic Resonance.* 43:249–258.
13. Hyde, J. S., J.-J. Yin, W. Froncisz, and J. B. Feix. 1985. Electron-electron double resonance (ELDOR) with a loop-gap resonator. *J Magnetic Resonance.* 63:142–150.
14. Popp, C. A., and J. S. Hyde. 1982. Electron-electron double resonance and saturation recovery studies of nitroxide electron and nuclear spin-lattice relaxation times and Heisenberg exchange rates: lateral diffusion in dimyristoyl phosphatidylcholine. *Proc. Natl. Acad. Sci. USA.* 79:2259–2263.
15. Eastman, M. P., G. V. Bruno, and J. H. Freed. 1970. ESR studies of Heisenberg spin exchange. III. An ELDOR study. *J. Chem. Phys.* 52:321–327.
16. Hyde, J. S., J. C. W. Chien, and J. H. Freed. 1968. Electron-electron double resonance of free radical in solution. *J. Chem. Phys.* 48:4211–4226.

17. Huisjen, M., and J. S. Hyde. 1974. A pulsed EPR spectrometer. *Rev. Sci. Instrum.* 45:669–675.
18. Träuble, H., and E. Sackmann. 1972. Studies of the crystalline-liquid crystalline phase transition of lipid model membranes. III. Structure of a steroid-lecithin system below and above the lipid-phase transition. *J. Am. Chem. Soc.* 94:4499–4510.
19. Rubenstein, J. L. R., B. A. Smith, and H. M. McConnell. 1979. Lateral diffusion in binary mixtures of cholesterol and phosphatidylcholines. *Proc. Natl. Acad. Sci. USA.* 76:15–18.
20. Demel, D. A., and B. De Kruyff. 1976. The function of sterols in membranes. *Biochim. Biophys. Acta.* 457:109–132.
21. Yeagle, P. L. 1985. Cholesterol and the cell membrane. *Biochim. Biophys. Acta.* 822:267–287.
22. Shimshick, E. J., and H. M. McConnell. 1973. Lateral phase separations in binary mixtures of cholesterol and phospholipids. *Biochem. Biophys. Res. Commun.* 53:446–451.
23. Rubenstein, J. L. R., J. C. Owicki, and H. M. McConnell. 1980. dynamic properties of binary mixtures of phosphatidylcholines and cholesterol. *Biochemistry.* 19:569–573.
24. Recktenwald, D. J., and H. M. McConnell. 1981. Phase equilibria in binary mixtures of phosphatidylcholine and cholesterol. *Biochemistry.* 20:4505–4510.
25. Percival, P. W., and J. S. Hyde. 1975. Pulsed EPR spectrometer, II. *Rev. Sci. Instrum.* 46:1522–1529.
26. Sugano, T., C. Mailer, and B. H. Robinson. 1987. Direct detention of very slow two-jump processes by saturation recovery electron paramagnetic resonance spectroscopy. *J. Chem. Phys.* 87:2478–2488.